

# Dynamics of optically-injected semiconductor nanolasers

J.-M. Sarraute<sup>a,b\*</sup>, K. Schires<sup>a</sup>, S. LaRochelle<sup>b</sup>, and F. Grillot<sup>a,c</sup>

<sup>a</sup>CNRS LTCI, Télécom Paristech, Université Paris-Saclay, 46 rue Barrault, 75013 Paris, France

<sup>b</sup>COPL, Université Laval, 2375 rue de la Terrasse, local 2104, G1V 0A6, Québec, Canada

<sup>c</sup>Center for High Technology Materials, University of New-Mexico, 1313 Goddard SE, Albuquerque, NM, United States

## ABSTRACT

We propose a novel rate equation model of an optically-injected semiconductor nanolaser based on an expression of the complex electric field including a novel spontaneous emission term. The latter takes into account the amplification of the zero-point energy of the field as well as the Purcell effect. The modulation response of the optically injection-locked nanolaser is studied for the first time using a small-signal analysis of the model. We then investigate the injection map of the nanolaser and study the 3-dB bandwidth of the nanolaser inside the locking region.

**Keywords:** Semiconductor lasers, injection-locking, modulation response, Purcell effect

## 1. INTRODUCTION

Semiconductor nanolasers are promising candidates for energy saving direct modulation applications in future optical communication networks.<sup>1,2</sup> Their attractiveness relies on the dimensions of the optical cavity, below the diffraction limit, which offers promises for a tighter integration on microelectronic chips. In addition, optical cavities of sub-wavelength dimensions can exhibit an enhanced spontaneous emission, quantified by the so-called Purcell factor. This factor is proportional to the ratio between the cubed lasing wavelength and the cavity volume<sup>3</sup> and becomes significant with cavity dimensions below the lasing wavelength. The increased spontaneous emission of nanocavities can also produce energy-efficient sources with ultra-low thresholds as opposed to edge-emitting semiconductor macrolasers. Last but not least, the enhanced carrier dynamics offer the possibility to achieve very large modulation bandwidth using direct current modulation. Although the technology has not yet reached a complete maturity, modulation bandwidths up to 60 GHz have already been predicted theoretically.<sup>4</sup> While such values are much larger compared to those achievable using edge-emitting semiconductor macrolasers, those are still lower than what could be achieved with external light modulators. However, optical injection-locking could be also used in a similar fashion as for edge-emitters in order to enhance the modulation bandwidth of directly-modulated nanolasers.<sup>5</sup> This work investigates the light injection from an external master laser into a slave nanolaser, which can lock onto the master wavelength under specific injection conditions. The direct-modulation response of the injection-locked laser then exhibits a resonance at the frequency detuning between the master and slave lasers, which allows reaching 3-dB bandwidths much larger than the free-running bandwidth of the slave laser. In this paper, the modulation dynamics of a nanolaser is investigated via a complex electric field model taking into account the amplification of the zero-point energy (ZPE) that depends on the Purcell factor. In particular, the effects of key parameters related to the spontaneous emission and the injected field on

---

\*jean-maxime.sarraute.1@ulaval.ca

the modulation bandwidth are discussed. Without optical injection-locking, simulations show 3-dB modulation bandwidths as large as 200 GHz. Under optical injection-locking, the main results point out that a very small injection ratio is sufficient to stably-lock the laser and to enhance the dynamics by several order of magnitude. This work is of prime importance for the development of novel energy-saving high-bandwidth directly-modulated optical sources for future high-speed optical networks.

## 2. SEMI-ANALYTICAL MODEL

The rate of spontaneous emission (SpE) arising in a sub-wavelength size cavity is controlled by the Purcell factor ( $F_p$ )<sup>4,6</sup> whose effect is inversely proportional to the cavity volume. However, in the case of a cavity with a gain medium, the SpE is also driven by the  $\beta$ -factor<sup>7</sup> which gives the fraction of SpE coupled to the fundamental optical lasing mode. As a strong contribution of SpE is expected in nanolasers, SpE noise must be fully taken into account in the field equation. Rate equations models dealing with optical injection often neglect SpE noise for analytical studies or include it only into the photon density equation<sup>8,9</sup> which implies that the emission noise field is not a complex field. While this approach is certainly valid for traditional edge-emitter macrolasers, where SpE can be neglected and only used in the rate equations as a seed for SpE or modal competition, it might not be the case anymore for a nanolaser. In this work, we define emission noise in the expression of the complex field in the form of amplification of a complex emission noise field. Previous studies have shown that the contributions of the Purcell and  $\beta$  factors are not independent and that a rigorous treatment of the SpE would require numerical calculations of the density of states.<sup>6,10,11</sup> Qualitatively, the  $\beta$ -factor cannot be seen as an independent parameter as it strongly depends on e.g. the Purcell factor, injection current and several other complex recombination mechanisms.<sup>12</sup> Using the  $\beta$ -factor as an independent knob does not allow to properly describe the cavity SpE rate which will strongly influence the corresponding nanolaser dynamics. Consequently, in this paper, a novel approach to describe the SpE is proposed via the implementation of a unique function  $f(F_p, \beta)$  which depends on both  $\beta$  and the Purcell factor  $F$ . While this function does not describe the individual contributions of the various physical phenomena behind noise emission and amplification, it allows studying the behavior of lasers with different amount of spontaneous emission using values derived from the literature. Future work will then concentrate on giving an expression of this functions based on the aforementioned physical parameters. As the aim of this work is to focus on the dynamical properties of an optically injection-locked nanolaser, the semi-analytical model described hereinafter directly includes the injected field. From the literature, it is known that the dynamics of a semiconductor laser operating under optical injection is described by a set a three differential rate equations with respect to the carrier density, photon density and phase respectively. First, the carrier density rate equation can be expressed as follows<sup>2,4,13,14</sup> :

$$\frac{dN_{e^-}}{dt} = \frac{J}{qV} - GN_\gamma - (1 - f(F_p, \beta)) \frac{N_{e^-}}{\tau_c}, \quad (1)$$

where  $N_{e^-}$  and  $N_\gamma$  are the carrier and photon densities, respectively,  $\tau_c$  the carrier lifetime and  $G$  the material gain.  $J$  represents the pump current,  $q$  the elementary charge and  $V$  the volume of the cavity. The term  $f(F_p, \beta)$  describes all the carriers lost by SpE. The unclamped material gain  $G$  is expressed as a logarithmic gain as follows:<sup>7</sup>

$$G = \frac{G_0}{1 + \varepsilon N_\gamma} \ln \left( \frac{N_{e^-} + N_s}{N_{tr} + N_s} \right) \quad (2)$$

where the compression factor  $\varepsilon$  accounting for gain nonlinearities is assumed to be zero in this work while  $N_{tr}$  is the carrier density at the optical transparency and  $N_s$  a fitting parameter. Both equations for photon density

and phase are extracted from the complex electrical field equation. In the particular case of an optically-injected semiconductor nanolaser for which the SpE can not be neglected, the novel expression of the complex electrical field equation is defined such that :

$$\frac{dE}{dt} = \left( \Gamma G - \frac{1}{\tau_p} \right) (1 + i\alpha_H) \frac{E}{2} + \Gamma f(F_p, \beta) \frac{E_0 N_{e^-}}{2N_\gamma \tau_c} + k_c A_{inj} - i\Delta\omega_{inj} E, \quad (3)$$

where  $E = E_0 e^{i\omega t}$  depicts the slave laser's electrical field,  $\Gamma$  the optical confinement factor and  $\Delta\omega_{inj}$  the frequency detuning between the slave and the master lasers. In Eq. 3 three different terms can be identified. Two describing the contribution of the stimulated emission to the slave laser's field e.g.  $E_{st} = \left( \Gamma G - \frac{1}{\tau_p} \right) (1 + i\alpha_H) \frac{E}{2}$  and the injected scalar field  $E_{inj} = k_c A_{inj} - i\Delta\omega_{inj} E$ . One describing the contribution of the SpE to the slave laser's field e.g.  $E_{sp} = \Gamma f(F_p, \beta) \frac{E_0 N_{e^-}}{2N_\gamma \tau_c}$ . Let us stress that the SpE term is written assuming Plank's definition of the ZPE.<sup>15</sup> Then, separating real and imaginary parts in Eq. 3 leads to a new set of rate equations both for photon density and phase :

$$\left\{ \begin{array}{l} \frac{dN_{e^-}}{dt} = \frac{J}{qV} - GN_\gamma - (1 - f(F_p, \beta)) \frac{N_{e^-}}{\tau_c}, \end{array} \right. \quad (4a)$$

$$\left\{ \begin{array}{l} \frac{dN_\gamma}{dt} = \left( \Gamma G - \frac{1}{\tau_p} \right) N_\gamma + 2N_\gamma \left( \Gamma f(F_p, \beta) \frac{N_{e^-}}{2N_\gamma \tau_c} + \eta \right) \cos(\phi), \end{array} \right. \quad (4b)$$

$$\left\{ \begin{array}{l} \frac{d\phi}{dt} = \left( \Gamma G - \frac{1}{\tau_p} \right) \frac{\alpha_H}{2} - \Delta\omega_{inj} - \left( \Gamma f(F_p, \beta) \frac{N_{e^-}}{2N_\gamma \tau_c} + \eta \right) \sin(\phi). \end{array} \right. \quad (4c)$$

From Eq. 4c, it is important to note that both  $\eta$  and  $E_{sp}/E_0$  do affect the phase.

In analogue modulation, a sinusoidal current variation is usually added to the continuous bias current. The modulation response of a semiconductor laser can thus be studied by solving the rate equations with a time-varying current. To this end, considering  $J$ ,  $N_{e^-}$ ,  $N_\gamma$ ,  $G$  and  $\phi$  as dynamical variable variables, one obtains,

$$\left\{ \begin{array}{l} dX = X_1 e^{i\omega t}, \end{array} \right. \quad (5a)$$

$$\left\{ \begin{array}{l} dG = \frac{G'_0}{1 + \varepsilon N_\gamma^0} dN_{e^-} - \frac{\varepsilon G}{1 + \varepsilon N_\gamma^0} dN_\gamma. \end{array} \right. \quad (5b)$$

Relationship (5a) shows that the small-signal condition leads to variations of all dynamical variables. Equation (5b) describes the derivation of equation (2) with respect to photon and carrier densities while the differential gain  $G'_0$  is defined as the partial derivative of the gain with respect to the carrier density :  $G'_0 = \partial G / \partial N_{e^-} = G_0 / (N_{e^-}^0 + N_s)$ . Finally,  $N_\gamma^0$  corresponds to the steady-state solutions with respect to the aforementioned rate equations in (4).

Using the small-signal analysis, the normalized transfer function  $|R_{NL}(f)|^2$  of the optically-injected nanolaser can be expressed as :

$$|R_{NL}(f)|^2 = \frac{\mathcal{A}_0^{NL2} \left( \mathcal{A}_1^{NL2} f^2 + \mathcal{C}_{1/2,1}^2 \right)}{\left[ \mathcal{A}_1^{NL} f - \mathcal{A}_3^{NL} f^3 \right]^2 + \left[ \mathcal{C}_{1/2,1} \mathcal{A}_0^{NL} - \mathcal{A}_2^{IO} f^2 \right]^2}, \quad (6)$$

TABLE 1: Material and Laser Parameters

Simulation parameters	Symbols	Value
Cavity length	$L$	$50 \times 10^{-9}$ m
Cavity height	$H$	$20 \times 10^{-9}$ m
Cavity width	$W$	$20 \times 10^{-9}$ m
Mirror reflectivity	$R_1 = R_2$	0.85
Steady-state optical gain	$G_0$	$1.54 \times 10^{13}$ s <sup>-1</sup>
Optical index	$n_g$	3.5
Carrier lifetime	$\tau_c$	$0.1 \times 10^{-9}$ s
Photon lifetime	$\tau_p$	$0.36 \times 10^{-12}$ s
Linewidth Enhancement Factor	$\alpha_H$	5
Coupling S-M factor	$k_c$	$1.39 \times 10^{13}$ s <sup>-1</sup>

with

$$\begin{aligned}
 \mathcal{A}_0^{\text{NL}} &= \frac{1}{8\pi^3} [\gamma^{\text{NL}} \mathcal{C}_{1,1} - \sigma \mathcal{D}_{3\phi,\alpha,1}], & \mathcal{A}_1^{\text{NL}} &= \frac{1}{4\pi^2} [\gamma^{\text{NL}} \mathcal{C}_{3/2,2} \cos(\phi) + \mathcal{C}_{1/2,1} \mathcal{C}_{1,1} - \sigma \mathcal{D}_{1,\cos(\phi)}], \\
 \mathcal{A}_2^{\text{NL}} &= \frac{1}{2\pi} [\gamma^{\text{NL}} + \mathcal{C}_{3/2} \cos(\phi)], & \mathcal{A}_{1'}^{\text{NL}} &= \frac{2\pi \mathcal{D}_{1,\cos(\phi)}}{\mathcal{D}_{3\phi,\alpha,1}}, & \mathcal{C}_{i,j} &= i \times \frac{\Gamma f(F_p, \beta) N_{e^-}^0}{\tau_c N_\gamma^0} + j \times \eta, \\
 \sigma &= \frac{1}{\tau_p} - \mathcal{C}_{1,2} \cos(\phi), & \mathcal{D}_{k,l} &= k \times \left( \gamma - \frac{1}{\tau_c} \right) + l \times \frac{f(F_p, \beta)}{\tau_c}, \\
 \gamma^{\text{NL}} &= \gamma - \frac{f(F_p, \beta)}{\tau_c}, & \mathfrak{Z}_{\phi,\alpha_H} &= \cos(\phi) - \alpha_H \sin(\phi), & \gamma &= \frac{1}{\tau_p} + G'_0 N_\gamma^0, & \eta &= k_c \sqrt{K}. \quad (7)
 \end{aligned}$$

Eq. 6 unveils a novel expression of the modulation transfer function of a semiconductor laser with a sub-wavelength cavity and operating under optical injection. Let us note that the transfer function of the optically-injected nanolaser is written in a conventional manner as a second order polynomial in  $f$  divided by a third order one which is similar to what is typically found in injection-locked macrolasers.<sup>16</sup> Besides, as shown in Eq. 7, all terms  $\mathcal{A}_i^{\text{NL}}$  depend on the  $\mathcal{C}_{i,j}$  coefficient, which becomes dominant as  $N_\gamma^0$  decreases. It is thus important to stress that  $N_\gamma^0$  decreases with  $I$  while the strength of the SpE  $f(F_p, \beta)$  increases. As stated in the introduction, nanolasers are expected to exhibit enhanced dynamical performances arising from the stronger contribution of  $f(F_p, \beta)$ . As a result, the next section investigates the modulation properties of a nanolaser operating with and without optical injection. In particular, the effects of the injection conditions and  $f(F_p, \beta)$  are simulated and discussed.

### 3. SIMULATION RESULTS

All the laser and material parameters used in the calculations are given in Tab. 1. Assuming a nanocavity such that  $V = H \times L \times W = 20 \times 50 \times 20$  nm<sup>3</sup>,<sup>3</sup> the condition  $V \ll \lambda^3$  is fulfilled for an operating wavelength at 1550 nm. Photon and carrier lifetime values are taken from.<sup>17</sup>

In order to check the validity of the model, we first investigate the light-current characteristic of the nanolaser and the evolution of the threshold current  $I_{\text{th}}$  with respect to  $f(F_p, \beta)$ . Fig 1 shows the steady-state photon density as a function of the pump current for different values of  $f(F_p, \beta)$ . As already reported in,<sup>13</sup> increasing the SpE induces a clear reduction of the laser's threshold current. For instance,  $I_{\text{th}}$  is about 1 mA for a sub-wavelength cavity with  $f(F_p, \beta) = 10^{-5}$  (green curve) whereas it decreases down to 20  $\mu$ A assuming the same

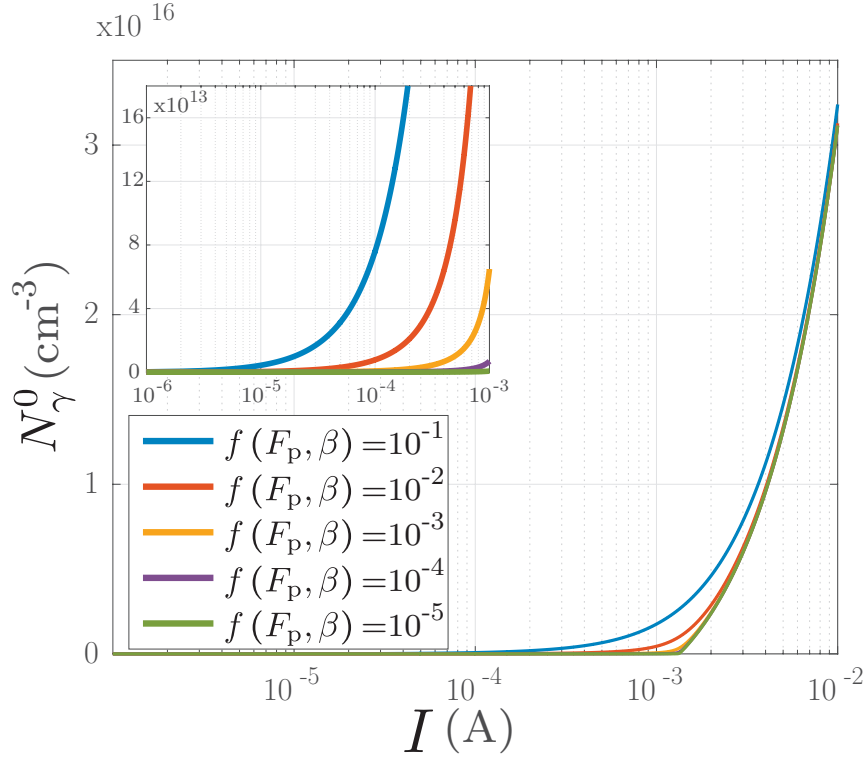


FIGURE 1: Evolution of the steady-state photon density into a sub-wavelength cavity as a function of the pump current  $I = J \cdot D$  for various values of  $f(F_p, \beta)$  ranging from  $10^{-5}$  to  $10^{-1}$ .

cavity but with  $f(F_p, \beta) = 0.1$  (blue curve). It is important to note that although a value of  $f(F_p, \beta) = 10^{-5}$  is not realistic for a nanocavity (sub-wavelength cavity dimensions induce a joint increase of both the  $\beta$  and Purcell factors leading to an SpE around  $10^{-3}$ ), the latter was used to qualitatively illustrate the effect on the lasing threshold. In the ultimate case of highly-enhanced SpE rates (not shown), simulations unveil the possibility to fully suppress the superlinearity of the laser characteristic around threshold, which can be meaningful for the realization of energy-efficient emitters.

Fig 2 depicts the calculated modulation responses without external optical injection ( $K = 0$ ) for different values of the pump current  $I$  and different SpE rates  $f(F_p, \beta)$ . As shown in Fig. 2(a) for  $f(F_p, \beta) = 0.1$  or in Fig. 2(b) for  $f(F_p, \beta) = 0.2$ , varying the pumping rate  $I$  does impact the modulation bandwidth. However, as opposed to edge-emitters which are pumped above threshold and for which the stimulated emission process is dominant, the behavior observed with nanolasers is different. Nanolasers can operate below threshold owing to their large SpE rates, hence a decrease of the pump below the threshold enhances the modulation dynamics. For instance, a modulation bandwidth as large as 200 GHz can theoretically be obtained for the laser under study with  $f(F_p, \beta) = 0.2$  and  $I = 1 \mu A$  ( $I < 0.05 \times I_{th}$ ). These conclusions are in a full agreement with prior arts published in reference<sup>3</sup> and confirm the validity of our model.

Fig. 3 describes the modulation response calculated for  $I < 0.05 \times I_{th}$  and  $f(F_p, \beta)$  ranging from 0.2 to 0.001. This data set illustrates the strong effect of the SpE term on the modulation dynamic of a semiconductor laser with sub-wavelength cavity. Indeed, even if the modulation bandwidth reaches 200 GHz for  $f(F_p, \beta) = 0.2$ , the latter decreases down to 10 GHz for  $f(F_p, \beta) = 0.05$  and does not exceed a few GHz for  $f(F_p, \beta) = 0.001$ . A recent study<sup>18</sup> has shown that  $f(F_p, \beta) = 0.1$  can be considered as a reasonable value for the SpE rate of a

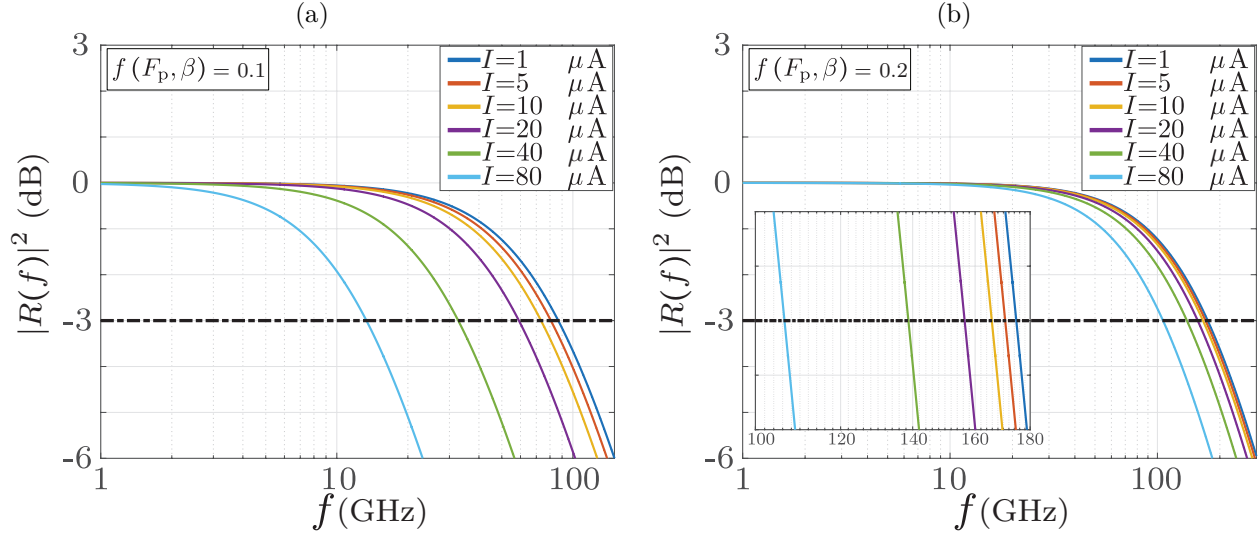


FIGURE 2: Modulation transfer functions of the free-running nanolaser calculated from 6 for  $I = \{1, 5, 10, 20, 40, 80\} \mu\text{A}$  with (a)  $f(F_p, \beta) = 0.1$  and (b)  $f(F_p, \beta) = 0.2$

sub-wavelength cavity.

In what follows, we consider a SpE rate such that  $f(F_p, \beta) = 0.001$ . For all values of the injection ratio  $K$ , the frequency detuning is chosen so that it corresponds to an operating condition within the stable-locking area hence between the saddle node and Hopf bifurcations. For each value of  $K$ , the frequency detuning  $\Delta f$  is computed by taking the average between saddle-node and Hopf bifurcation lines following the expression  $\Delta f(K) = (\text{SN}(K) + \text{Hp}(K))/2$ . Each value of  $\Delta f$  is then normalized by the relaxation oscillation frequency (ROF)  $f_R^{f(F_p, \beta)}$  whose expression is given by :

$$f_R^{f(F_p, \beta)} = \frac{1}{4\pi^2} \left[ \frac{\Gamma f(F_p, \beta) N_e^0}{\tau_c N_\gamma^0} \left( \gamma - \frac{1 - 2f(F_p, \beta)}{\tau_c} \right) + \frac{1}{\tau_p} \left( \gamma + \frac{1 - f(F_p, \beta)}{\tau_c} \right) \right] \quad (8)$$

Although the ROF is not visible in the previous figures due to the large damping factor associated to the very low photon lifetime, sub-wavelength cavities behave similarly to conventional ones<sup>3</sup> and a ROF can be defined. The expression of  $f_R^{f(F_p, \beta)}$  is extracted from the normalized transfer function under the free-running case without optical injection. For the laser under study, the ROF which depends on the SpE rate and the pump current is found to be about 75 GHz for  $f(F_p, \beta) = 0.2$  and  $I = 1 \mu\text{A}$  ( $I < 0.05 \times I_{\text{th}}$ ). Fig. 4 in red shows the free-running modulation response calculated at  $I = 1 \mu\text{A}$  whereas those in blue, green and brown are obtained assuming different optical injection conditions, i.e.  $K = 8, 0.1, 10^{-5}$  with  $\Delta f/f_R^{f(F_p, \beta)} = \{-1.699, -0.850, -0.060, -0.004\}$ . In addition, for each  $\{K, \Delta f/f_R^{f(F_p, \beta)}\}$ , simulations are performed for  $f(F_p, \beta) = 0.1$  (solid lines) and  $f(F_p, \beta) = 0.2$  (dotted lines). Results reveal that there is no need to use a strong injection strength as what is necessary for a macrolaser. With a nanolaser, a small injection ratio is enough to stably-lock the laser onto the master as well as to substantially enhance the modulation dynamics. For instance, with  $K = 10^{-5}$ , the theoretical modulation bandwidth can already be as high as 800 GHz. Owing to the stimulated photons that are injected into the laser cavity, the bandwidth scales up with the injection strength even if the nanolaser is pumped below threshold. Finally, let us stress that although a large linewidth enhancement factor is considered, the calculated locking map (not shown) appears rather symmetrical which differs from what is normally observed in injection-locked macrolasers.

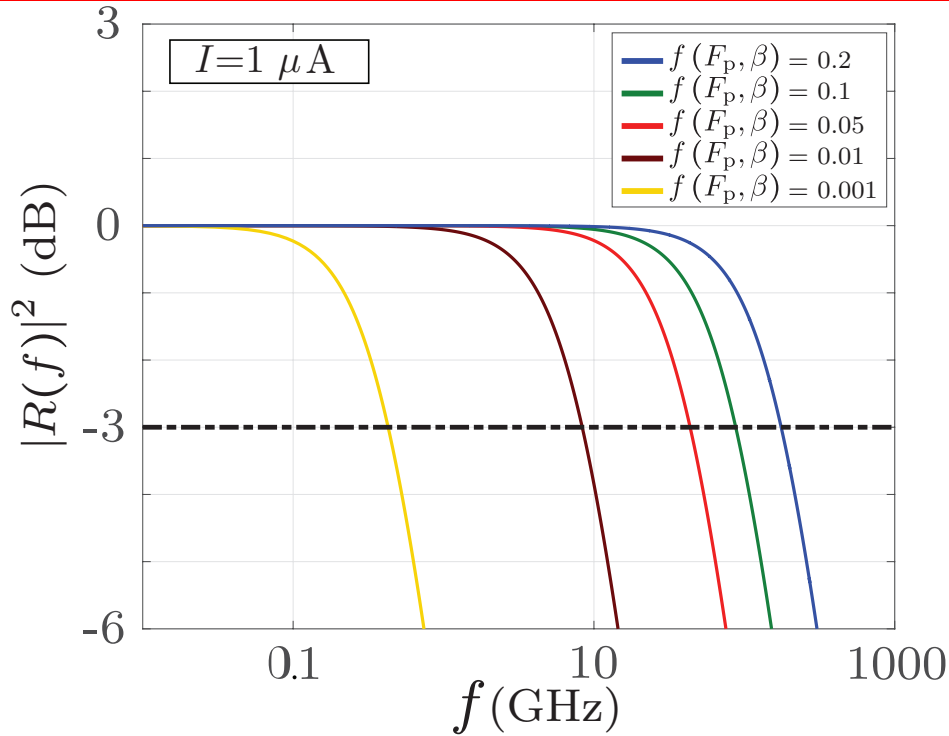


FIGURE 3: Modulation transfer functions of the free-running nanolaser calculated for 6,  $f(F_p, \beta) = \{0.2, 0.1, 0.05, 0.01, 0.001\}$  and with  $I=1 \mu\text{A}$

#### 4. CONCLUSIONS

This work investigates the modulation dynamics of a nanolaser with a novel rate equation model taking into account the ZPE energy. Without optical injection-locking, simulations show the high potential in using a quantum-confined cavity with enhanced spontaneous emission rates. Under the free-running case, 3-dB modulation bandwidths as large as 200 GHz are predicted below the laser's threshold. Under optical-injection, simulations point out that a stably-locked nanolaser can exhibit large modulation dynamics at injection rates that are by far much smaller than those used in edge-emitting macrolasers. Because a large bandwidth enhancement can thus be reached with low injected light, we believe that these results will prove useful for the development of energy-saving directly-modulated optical sources for future high-speed optical networks.

#### ACKNOWLEDGMENTS

This work is supported by the Institut Mines-Telecom, the European Office of Aerospace Research and Development under Grant FA9550-15-1-0104 as well as by the NSERC through the CRC in Advanced Photonics Technologies for Communications.

#### REFERENCES

- [1] T. Baba, "Photonic crystals and microdisk cavities based on gainasp-inp system," *Selected Topics in Quantum Electronics, IEEE Journal of* **3**(3), pp. 808–830, 1997.
- [2] K. A. Shore, "Modulation bandwidth of metal-clad semiconductor nanolasers with cavity-enhanced spontaneous emission," *Electronics letters* **46**(25), pp. 1688–1689, 2010.

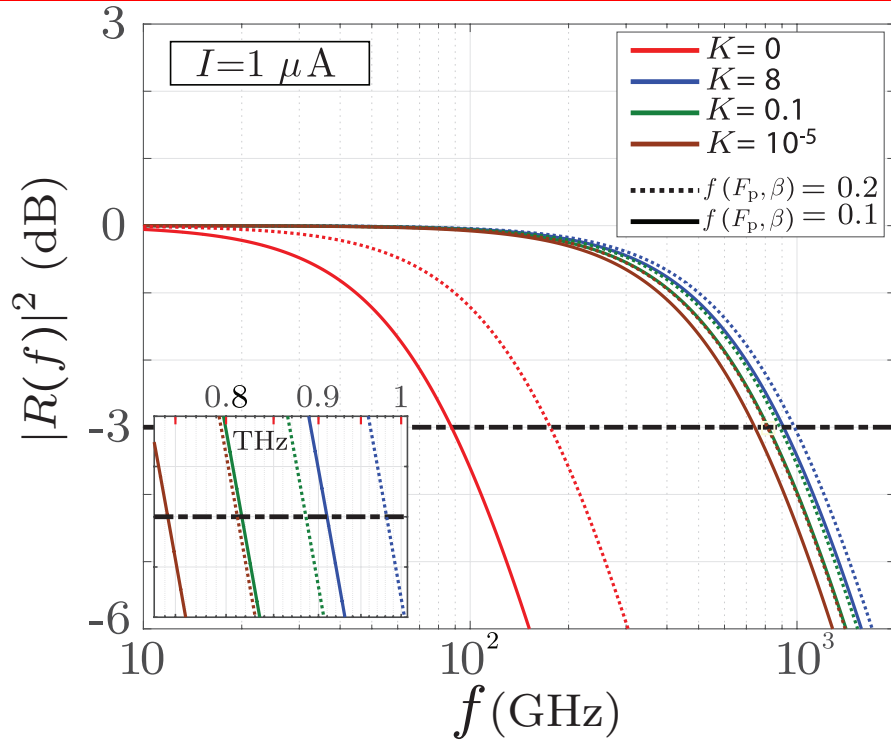


FIGURE 4: Modulation transfer functions of the optically injection-locked nanolaser calculated from 6 for  $K = \{0, 8, 0.1, 10^{-5}\}$  and  $\Delta f/f_R^{f(F_p, \beta)} = \{-1.699 - 0, 850, -0.060, -0.004\}$  with  $f(F_p, \beta) = \{0.1, 0.2\}$  and  $I = 1\mu\text{A}$ .

- [3] E. K. Lau, A. Lakhani, R. S. Tucker, and M. C. Wu, "Enhanced modulation bandwidth of nanocavity light emitting devices," *Optics Express* **17**(10), pp. 7790–7799, 2009.
- [4] Z. A. Sattar and K. A. Shore, "External optical feedback effects in semiconductor nanolasers," *Selected Topics in Quantum Electronics, IEEE Journal of* **21**(6), pp. 1–6, 2015.
- [5] T. B. Simpson, J. Liu, and A. Gavrielides, "Bandwidth enhancement and broadband noise reduction in injection-locked semiconductor lasers," *Photonics Technology Letters, IEEE* **7**, pp. 709–711, July (1995).
- [6] T. Suhr, N. Gregersen, K. Yvind, and J. Mørk, "Modulation response of nanoleds and nanolasers exploiting purcell enhanced spontaneous emission," *Optics express* **18**(11), pp. 11230–11241, 2010.
- [7] L. Coldren and S. Corzine, *Diode Lasers and Photonic Integrated Circuits*, Wiley Series in Microwave and Optical Engineering, Wiley, 1995.
- [8] F. Mogensen, H. Olesen, and G. Jacobsen, "Locking conditions and stability properties for a semiconductor laser with external light injection," *Quantum Electronics, IEEE Journal of* **21**(7), pp. 784–793, 1985.
- [9] A. Valle, M. Sciamanna, and P. K., "Irregular pulsating polarization dynamics in gain-switched vertical-cavity surface-emitting lasers," *Quantum Electronics, IEEE Journal of* **44**(2), p. 136, 2008.
- [10] Q. Gu, B. Slutsky, F. Vallini, J. S. Smalley, M. P. Nezhad, N. C. Frateschi, and Y. Fainman, "Purcell effect in sub-wavelength semiconductor lasers," *Optics express* **21**(13), pp. 15603–15617, 2013.
- [11] T. Suhr, N. Gregersen, M. Lorke, and J. Mørk, "Modulation response of quantum dot nanolight-emitting-diodes exploiting purcell-enhanced spontaneous emission," *Applied Physics Letters* **98**(21), p. 211109, 2011.
- [12] J. M. Gerard and B. Gayral, "InAs quantum dots : artificial atoms for solid-state cavity-quantum electrodynamics," *Physica E : Low-dimensional Systems and Nanostructures* **9**(1), pp. 131–139, 2001.



- [13] C. Ning, "What is laser threshold?," *Selected Topics in Quantum Electronics, IEEE Journal of* **19**(4), pp. 1503604–1503604, 2013.
- [14] J. B. Khurgin and G. Sun, "Comparative analysis of spasers, vertical-cavity surface-emitting lasers and surface-plasmon-emitting diodes," *Nature Photonics* **8**(6), pp. 468–473, 2014.
- [15] M. Planck, *Eine neue Strahlungshypothese*, Vieweg, 1911.
- [16] N. A. Naderi, "Quantum dot gain-lever laser diode," Master's thesis, University of New Mexico.
- [17] Z. Abdul Sattar, N. Ali Kamel, and K. Shore, "Optical injection effects in nanolasers," *Quantum Electronics, IEEE Journal of* **52**, pp. 1–8, Feb 2016.
- [18] N. Gregersen, T. Suhr, M. Lorke, and J. Mørk, "Quantum-dot nano-cavity lasers with purcell-enhanced stimulated emission," *Applied Physics Letters* **100**(13), p. 131107, 2012.